Changes in Gray Matter Volume and White Matter Microstructure in Adolescents with Obsessive-Compulsive Disorder

Mojtaba Zarei, David Mataix-Cols, Isobel Heyman, Morgan Hough, Joanne Doherty, Linda Burge, Louise Winmill, Sunita Nijhawan, Paul M. Matthews, and Anthony James

Background: There is a paucity of neuroimaging data in pediatric-onset obsessive-compulsive disorder (OCD). This multimodal neuroimaging study aimed to identify structural gray (GM) and white matter (WM) microstructure changes in pediatric OCD.

Methods: We obtained structural and diffusion tensor magnetic resonance images from 26 OCD patients and 26 matched healthy adolescents. We carried out a series of image analyses including, volumetric and shape analysis of subcortical gray structures, as well as voxel-based morphometry on GM volume and fractional anisotropy of the WM.

Results: Patients had increased GM volume in the caudate bilaterally and right putamen. Shape analyses revealed specific hypertrophy of the dorsal caudate in pediatric OCD. The striatum was larger in healthy boys compared with healthy girls, whereas such a gender effect was not seen in the OCD group. OCD subjects showed higher fractional anisotropy values in left inferior longitudinal fasciculus, bilateral superior longitudinal fasciculus, right inferior fronto-occipital fasciculus, bilateral corticospinal tract, corpus callosum splenium and genu, bilateral forceps major, bilateral forceps minor, left cingulum, and right uncinate fasciculus. OCD symptom severity was positively correlated with GM volume in right insula, posterior orbitofrontal cortex, brainstem, and cerebellum and inversely correlated with widespread reduction in cortical GM volume. Furthermore, symptom severity positively correlated with increased WM fractional anisotropy in various WM tracts, including the anterior limb of the internal capsule.

Conclusions: Adolescents with OCD had a wide range of GM and WM changes compared to healthy control subjects that are broadly consistent with those identified in the adult OCD literature but are more extensive.

Obsessive-compulsive disorder (OCD) is characterized by repetitive unwanted thoughts (obsessions) or repetitive actions (compulsions). OCD is relatively common, affecting approximately 2% of adults (1). It is relatively rare in the very young, but its prevalence increases to adult rates at puberty and affects around 1% of children and adolescents overall (2). Early-onset OCD appears to include a substantial proportion of individuals who, when treated, experience symptom remission before early adulthood (3). Pediatric OCD differs from adulthood OCD in terms of its gender ratio (more frequent in boys) and patterns of comorbidity (younger patients are more likely to present with comorbid tic disorders and attention-deficit/hyperactivity disorder). Furthermore, early-onset OCD exhibits greater familial loading and heritability than adult-onset OCD, indicating a stronger genetic component (3,4). There is some inconsistent evidence indicating that patients with early onset may be less likely to respond to serotonin reuptake inhibitors (5,6), although these findings may be confounded by the presence of tic-related cases (3,7). Conversely, early- and late-onset cases seem to benefit equally from cognitive-behavior therapy (8). Thus, whether early-onset OCD constitutes a neurobiologically or clinically different subtype of OCD remains a matter of debate (3).

Cumulative evidence from 2 decades of functional and structural neuroimaging research in adult OCD has implicated specific cortico-striato-thalamic circuits in the mediation of symptoms (9–13). A relatively small number of neuroimaging studies have been conducted in children and adolescents with OCD (14). To a large extent, their findings have been consistent with those of the adult OCD literature and implicated components of same the cortico-striato-thalamic loops. However, some differences may also exist (14–16), which may either reflect brain maturation or simply methodological issues. Clearly, there is a need to increase the neuroimaging evidence base for pediatric OCD. In particular, more studies on white matter integrity are needed to understand the potential alterations in short- and long-range tracts that interconnect discrete brain regions. Although a handful of diffusion tension imaging (DTI) studies have been conducted in adult OCD (17–19), to date, no studies have examined white matter microstructure in pediatric OCD.

The current multimodal neuroimaging study employed a range of structural neuroimaging methods in the same participants, including volumetric and shape analyses of subcortical gray matter structures as well as voxel-based morphometry on gray matter volume and fractional anisotropy of white matter in a well-characterized sample of children and adolescents with OCD and matched control subjects. We tested the hypothesis that adolescents with OCD would display alterations in the same the cortico-striato-thalamic loops and white matter tracts previously implicated in adult OCD. We hoped the results would shed some light on the question of whether pediatric OCD is a neurobiologically meaningful variant of OCD.

Table 1. Demographic and Clinical Characteristics of the Sample

	OCD Patients ($n = 26$)	Control Subjects ($n = 26$)	Statistic	p Value
Sex (male/female)	14/12	14/12	$\chi^2 = .0$	1.0
Age (mean $\pm$ SD)	16.6 $\pm$ 1.5	16.5 $\pm$ 1.4	$t_{50} = .09$	.93
Handedness (left/right)	3/23	3/23	$\chi^2 = .0$	1.0
Age at Onset of Symptoms in Years (mean $\pm$ SD)	11.2 $\pm$ 2.8	—		
Disease Duration in Years (mean $\pm$ SD)	5.3 $\pm$ 3.4	—		
CY-BOCS—Obsessions (mean $\pm$ SD)	9.7 $\pm$ 3.9	—		
CY-BOCS—Compulsions (mean $\pm$ SD)	9.8 $\pm$ 3.9			
YBOCS—Total (mean $\pm$ SD)	19.5 $\pm$ 7.6			
BDI Score (mean $\pm$ SD)	9.8 $\pm$ 7.3	—		
Full-Scale IQ (mean $\pm$ SD)	109.4 $\pm$ 12.5	110.8 $\pm$ 10.3	$t_{46} = .43$	.66
Cerebrospinal Fluid, mm³ (mean $\pm$ SD)	24,875 (9717)	24,231 (12,308)	$t_{49} = .2$	.83
Total Gray Matter, mm³ (mean $\pm$ SD)	910,027 (52,578)	877,379 (41,505)	$t_{50} = 2.48$	.02[a]
Total White Matter, mm³ (mean $\pm$ SD)	812,086 (55,541)	823,093 (63,525)	$t_{50} = .67$	.50
Total Brain Volume, mm³ (mean $\pm$ SD)	1,721,753 (63,662)	1,7004,113 (57,277)	$t_{50} = 1.2$	.21
Medication	(15/26)			
Fluoxetine	11			
Sertraline	3			
Citalopram	1			
Aripiprazole	1			

BDI, Beck Depression Inventory; CY-BOCS, Children's Yale–Brown Obsessive Compulsive Scale; OCD, obsessive-compulsive disorder.

[a]Significant group difference.

Methods and Materials

Participants

Twenty-six adolescents (14 males, 12 females) aged 12 to 18 years were recruited from the Highfield Adolescent Unit, Oxford, and the national specialist pediatric OCD clinic at the Maudsley Hospital, London. All children underwent a detailed clinical assessment carried out by psychiatrists and psychologists experienced in the assessment of pediatric OCD. Diagnoses were made from the clinical history and the results of a structured interview with the Children's Yale–Brown Obsessive Compulsive Scale (CY-BOCS [20]), according to ICD-10 criteria. Mean pretreatment score on the CY-BOCS was 20.5 (range 12–33), indicating moderate symptom severity. Exclusion criteria included intellectual disability, comorbid tic disorders (including Tourette syndrome), autism-spectrum disorder, attention-deficit/hyperactivity disorder, affective disorders or other anxiety disorders. The main demographic and clinical characteristics of the sample are shown in Table 1. The majority of participants in the OCD group ($n = 16$) were being treated with a selective serotonin reuptake inhibitor (SSRI), with a mean duration of treatment of 5 months (range 2–12); one child was on two SSRIs at assessment time (being crossed over from one drug to the other), and another was on an SSRI augmented with a dopamine antagonist (aripiprazole). All patients received cognitive-behavioral therapy (mean 8 sessions, range 4–10) but remained at least moderately impaired at the time of the scan. The control group comprised 26 sex, age, handedness, and IQ-matched healthy control subjects screened using the Child Behavior Checklist and the CY-BOCS. Intellectual ability was estimated with the Wechsler Abbreviated Scale of Intelligence (21). The study was approved by the local ethics committees, and written informed consent was obtained from all participants and parents.

Image Acquisition

All participants underwent whole-brain T1-weighted and diffusion-weighted scanning using the same 1.5-T Sonata MR imager (Siemens, Erlangen, Germany) with a standard quadrature head coil and maximum 40 mT m-1 gradient capability. All subjects were scanned with a three-dimensional T1-weighted fast low angle shot magnetic resonance imaging) sequence using the following parameters: coronal orientation, matrix 256 $\times$ 256, 208 slices, 1 $\times$ 1 mm² in-plane resolution, slice thickness 1 mm, echo time/repetition time = 5.6/12 msec, flip angle $\alpha = 19°$.

Diffusion-weighted images were obtained on the adolescent cohort (first and second time points) using echo-planar imaging (spin-echo echo planar imaging, echo time/repetition time = 89/8500 msec, 60 axial slices, bandwidth = 1860 Hz/vx, voxel size 2.5 $\times$ 2.5 $\times$ 2.5 mm³) with 60 isotropically distributed orientations for the diffusion-sensitizing gradients at a b-value of 1000s mm² and 5 b = 0 images. To increase signal-to-noise ratio, scanning was repeated three times, and all scans were corrected for head motion and eddy currents using affine registration before being averaged.

Image Analyses

The entire image analysis in this study was carried out using different tools from FMRIB Software Library (FSL) software (Oxford Centre for Functional Magnetic Resonance Imaging of the Brain Software Library, http://www.fmrib.ox.ac.uk/fsl) (22). We used a combination of structural and diffusion tensor image analysis. Brief description of each step is described in the following sections.

Voxel-Wise Morphometry

Structural data were analyzed with FSL-VBM, a voxel-based morphometry (VBM)-style analysis (23,24) carried out with FSL tools (22). First, structural images were brain-extracted using BET (25). Next, tissue-type segmentation was carried out using FAST4 (26). The resulting gray-matter partial volume images were then aligned to Montreal Neurological Institute (MNI) 152 standard space using the affine registration tool FMRIB's Linear Image Registration Tool (FLIRT) (27,28), followed by nonlinear registration using FMRIB's Nonlinear Image Registration Tool (FNIRT) (29,30), which uses a b-spline representation of the registration warp field (31). The resulting images were averaged to create a study-specific template, to which the native gray matter images were then nonlinearly reregistered. The

registered partial volume images were then modulated (to correct for local expansion or contraction) by dividing by the Jacobian of the warp field. The modulated segmented images were then smoothed with an isotropic Gaussian kernel with a sigma of 3 mm. Finally, voxel-wise general linear modeling (GLM) was applied using permutation-based nonparametric testing and threshold-free cluster enhancement, correcting for multiple comparisons across space using false discovery rate (FDR) method (32).

Shape Analysis of the Basal Ganglia

FIRST (part of FSL) was used to segment automatically subcortical gray matter structures, including nucleus accumbens, caudate, putamen, and pallidum (33). In brief, FIRST is a probabilistic adaptation of the active appearance model (34). The method is informed by the shape and intensity variations of a structure from a training set for the purpose of automatically segmenting the structure. A multivariate Gaussian model of vertex location and intensity variation is used and is based on having point correspondence across subjects (same number and labeling of vertices across subjects). The necessary correspondence is imposed during the parameterization of the labeled images with a deformable model. The model is fit to new images by maximizing the posterior probability of shape given the observed intensities.

To assess any changes in the shape of basal ganglia, we used vertex-wise analysis, which is part of the previously described FIRST tool (33). In brief, FIRST creates a surface mesh for each subcortical structure using a deformable mesh model. The mesh is composed of a set of triangles, and the apex of adjoining triangles is called a vertex. The number of vertices for each structure is fixed so that corresponding vertices can be compared across individuals and between groups. Although the vertices retain correspondence, the surfaces reside in the native image space and thus have an arbitrary position. Therefore, the surfaces must all be aligned to a common space before investigating any group differences. The mean surface from the FIRST models (in MNI152 space) is used as the target to which surfaces from the individual subjects are aligned after removal of rotation and translation. Group comparisons of vertices were carried out using F statistics controlling for the participants' age and gender (33).

Diffusion Tensor Imaging

BET was used for brain extraction of the T1-weighted images, and FLIRT was used to perform affine alignment of the diffusion and T1-weighted images. Effects of eddy current and head motion were reduced by registering all the diffusion-weighted images to a non-diffusion-weighted reference image using an affine, 12 degrees of freedom registration. The second and third DTI volumes were registered into the first volume and averaged to increase signal to noise ratio.

Voxel-wise statistical analysis of the fractional anisotropy (FA) data was carried out using Tract-Based Spatial Statistics (TBSS) (35), part of FSL. In brief, FA images were created by fitting a tensor model to the raw diffusion data using FMRIB Diffusion Tool (part of FSL), and then brain-extracted using BET (25). All subjects' FA data were then aligned into a common space using FNIRT, the nonlinear registration tool from FSL, which uses a b-spline representation of the registration warp field (30). Next, the mean FA image was created and thinned to create a mean FA skeleton that represents the centers of all tracts common to the group. Each subject's aligned FA data were then projected onto this skeleton, and the resulting data were fed into voxel-wise cross-subject statistics. Finally, voxel-wise GLM was applied using permutation-based nonparametric testing and threshold-free cluster enhancement, correcting for multiple

comparisons across space using false discovery rate (FDR) method (32). The thresholded statistical images were "thickened," filling them out into the local "tracts" seen in the mean FA map.

Behavior-Imaging Correlations

We studied association between symptom severity, as measured with the CY-BOCS and gray matter volume/fractional anisotropy. We used a linear regression model to examine if gray matter volume or FA value would predict CY-BOCS scores while controlling for age, gender, and depression scores. The result was corrected for multiple comparisons using false discovery rate ($p < .01$) after applying threshold-free cluster enhancement (36).

Results

Gray Matter Volume and White Matter Microstructure

VBM group comparison of regional gray matter volume showed that OCD subjects had greater gray matter volume in caudate nuclei, right posterior putamen, and right globus pallidus than controls (Figure 1 and Table S2 in Supplement 1). Group comparison of FA maps using TBSS showed that OCD participants had higher FA in left inferior longitudinal fasciculus (ILF), bilateral superior longitudinal fasciculus (SLF), right inferior fronto-occipital fasciculus (IFOF), bilateral corticospinal tract (CST), corpus callosum splenium and genu, bilateral forceps major, bilateral forceps minor, left cingulum, and right uncinate fasciculus (Figure 1 and Table S1 in Supplement 1).

To examine whether the observed group difference was driven by medication use, we carried out a region of interest analysis of the significant regions that were found in whole brain analysis and compared medicated ($n = 16$) with unmedicated ($n = 10$) OCD participants using TBSS and FSLVBM. This analysis showed no difference between groups, suggesting that there was no significant effect of medication on regional gray matter volume or FA changes (data not shown).

### Shape Analysis Using Vertex-Wise Comparisons

Vertex-wise shape analysis showed patches of hypertrophy on the rostral-ventral aspect of caudate nucleus, medial aspects of putamen and pallidum, as well as lateral aspect of putamen in OCD when compared with control subjects (Figure 2). However, only the area on the dorsal aspect of left caudate survived correction for multiple comparisons using FDR.

Further shape analyses by sex within the control group showed that the medial aspect of right putamen and right pallidum were larger in healthy boys compared with healthy girls. These changes survived FDR correction for multiple comparisons. This gender effect was not seen in OCD participants (Figure 2).

Correlations with Symptom Severity

Voxel-wise assessment of the relationship between total CY-BOCS severity scores and gray matter volume/white matter FA was conducted. Symptom severity correlated negatively with widespread reduction in cortical gray matter volume in ventromedial (anterior orbitofrontal), ventrolateral (pars opercularis), dorsolateral prefrontal cortex, medial and anterior temporal cortex, central operculum, and brainstem, as well as the parietal and occipital regions and right thalamus. A few brain regions showed a positive correlation between the gray matter volume and symptom severity. These included bilateral cerebellar cortex, right insula, and left posterior orbitofrontal cortex, extending to the subgenual cingulate cortex and the ventral striatum (Figure 1 and Table S2 in Supplement 1).

Symptom severity was positively correlated with white matter FA in various regions, particularly in the left uncinate fasciculus,
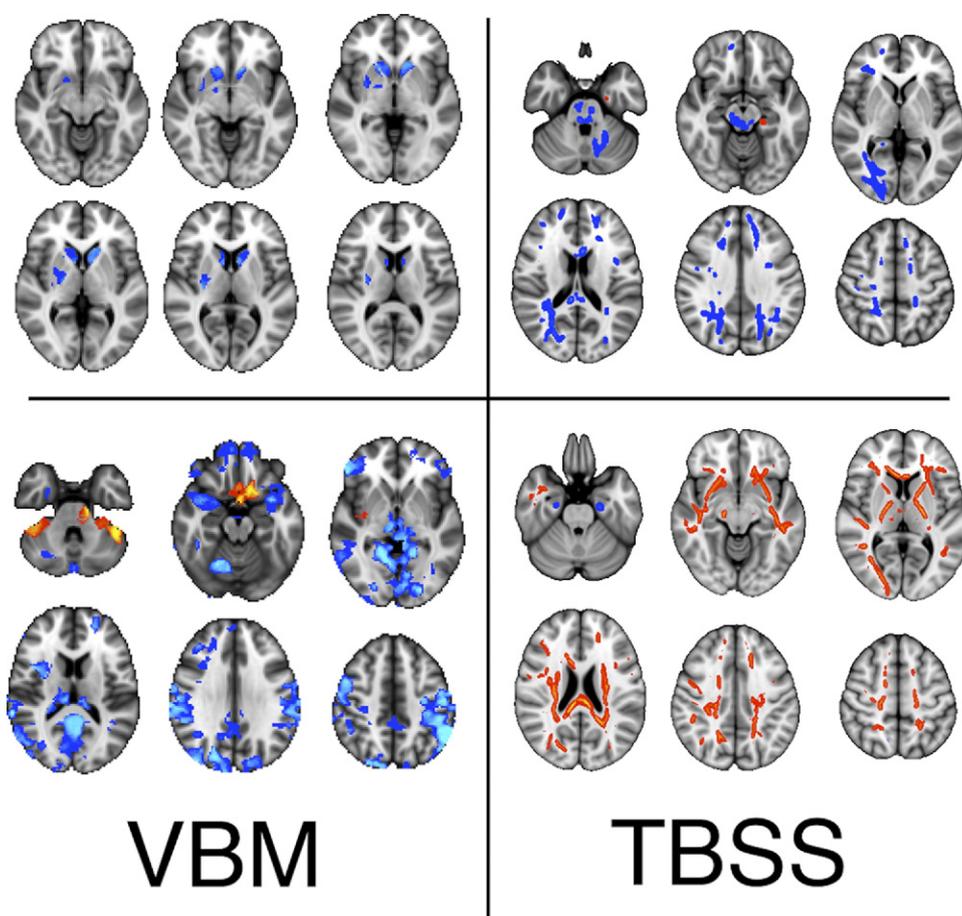
Figure 1. Top left panel: voxel-based morphometry (VBM) analyses. Red-yellow indicates control greater than obsessive-compulsive disorder (OCD) subjects, and dark/light blue indicates OCD greater than control subjects; color coding indicates 1-*p* value range .95–1.0. Bottom left panel: relationship of gray matter changes with symptom severity (Children's Yale–Brown Obsessive Compulsive Scale scores) in OCD. Red-yellow indicates positive correlation, and dark/light blue indicates negative correlation. Top right panel: Tract-Based Spatial Statistics analyses (TBSS). Red-yellow indicates control greater than OCD subjects, and dark/light blue indicates OCD greater than control subjects; color coding indicates 1-*p* value range .95–1.0. Bottom right panel: Relationship of white matter fractional anisotropy changes with Children's Yale–Brown Obsessive Compulsive Scale symptom severity in OCD. Red-yellow indicates positive correlation and dark/light blue indicates negative correlation. See Tables S1 and S2 in Supplement 1 for coordinates.

corticospinal tract, superior longitudinal fasciculus, forceps major, forceps minor, superior corona radiata, splenium, anterior thalamic radiation, posterior limb of the internal capsule (Figure 1 and Table S2 in Supplement 1). Interestingly, the increased FA within the posterior limb of internal capsule extended all the way to the motor cortex bilaterally, suggesting that it is mostly related to corticospinal tracts. There was a significant negative correlation in left hippocampal cingulum adjacent to entorhinal cortex bilaterally.

Discussion

This study uniquely employed multimodal structural neuroimaging including high resolution T1 and DTI to characterize the extent of gray and white matter brain abnormalities in pediatric OCD. Voxel-based morphometry revealed increased regional gray matter volume in the caudate nucleus bilaterally and right putamen. Furthermore, vertex-wise shape analysis showed hypertrophy on the rostral-ventral aspect of caudate nucleus, medial aspects of putamen and pallidum, as well as lateral aspect of putamen, although only the area on the dorsal aspect of left caudate survived correction for multiple comparisons. The basal ganglia have long been hypothesized to play a key role in the mediation of obsessive-compulsive symptoms (37). Indirect evidence is available from focal lesion studies, disorders of known basal ganglia pathology, and, more recently, from neuroimaging studies. Indeed, several meta-analyses of both structural (11,12,38) and functional (13,39) neuroimaging studies have confirmed that OCD is characterized by increased regional gray matter volumes and metabolism/activation in the striatum. Furthermore, a recent meta-analysis of VBM studies reported that studies that included individuals with more severe

OCD were significantly more likely to report increased gray matter volumes in the striatum (11).

The results also revealed an abnormal laterality pattern in which the medial aspect of right putamen and right pallidum were larger in healthy boys compared with healthy girls, whereas such gender effect was not seen in the OCD group. Similar findings were reported in adult OCD (40), as well as in other OCD-related disorders such as Tourette's disorder (41,42) and body dysmorphic disorder (43). Taken together, the results suggest developmental abnormalities in the basal ganglia in pediatric OCD, which are consistent with prevailing cortico-striato-thalamic models of the disorder (9,10,13,44).

Symptom severity (CY-BOCS score) was positively correlated with gray matter volume in right insula and left posterior orbitofrontal cortex, extending to the subgenual cingulate cortex and the ventral striatum, cerebellum, and the brainstem. Paralimbic brain regions have consistently been implicated in OCD and other anxiety disorders in the adult neuroimaging literature (44). The finding of a positive correlation between symptom severity and increased gray matter in the brainstem is consistent with a previous study that reported increased gray matter volume in the midbrain in adults with OCD (45). Rauch *et al.* (44) found a strong correlation between relative regional cerebral blood flow in the brainstem during symptom provocation and subjective anxiety scores across various anxiety disorders, including OCD. Thus, these findings may reflect nonspecific brain correlates of anxiety in pediatric OCD.

Symptom severity was also negatively correlated with gray matter volume in ventromedial (anterior orbitofrontal), ventrolateral (pars opercularis), and dorsolateral prefrontal, and medial and an-

Figure 2. Vertex-wise shape analysis. Images in the left column show gender effect in control, and in the middle column show (absence of) gender effect in obsessive-compulsive disorder (OCD) controlling for age. Right column shows vertex-wise group comparison, OCD greater than control group controlling for age, gender, and Children's Yale–Brown Obsessive Compulsive Scale severity score. These figures show areas of hypertrophy in the dorsal caudate and medial aspect of left putamen and pallidum in OCD compared with control subjects (*F* values are corrected; degrees of freedom = 3,46). Ant., anterior; Post., posterior; Rt., right; Lt., left; stat., statistic.

terior temporal, as well as parietal and occipital regions and thalamus. The most widely accepted neuroanatomic model of OCD proposes the involvement of a direct and an indirect cortico-striato-thalamic pathway (46–48). In the direct pathway excitatory glutamatergic neurons project to the striatum, which in turn activate inhibitory gamma-aminobutyric acidergic neurons to modulate the internal part of the globus pallidus. This results in a decreased inhibition (disinhibition) of the thalamus and thus an increased excitatory effect on the ventral prefrontal cortex. In the indirect pathway, the striatum projects an inhibitory signal to the external part of the globus pallidus and the subthalamic nucleus, sending an excitatory signal to the internal part of the globus pallidus. The net effect is an increased inhibition of the thalamus and decreased excitation on the dorsal prefrontal cortex. On the basis of functional neuroimaging results, imbalance between these frontal-striatal circuits might mediate OCD symptomatology (9). The results of functional neuroimaging studies in OCD broadly support this view, showing increased activation of limbic and ventral frontal-striatal regions at rest and in response to disease-relevant information and decreased responsiveness of dorsal frontal-striatal regions during executive performance (49,50). Furthermore, a resting-state functional connectivity study found significantly increased functional connectivity in ventral frontal-striatal networks, coupled with de-

creased connectivity in dorsal frontal-striatal networks in adult OCD patients compared with controls (51). Recent insights from cognitive and affective neuroscience suggest complex interactions between the dorsal and the ventral frontal-striatal circuits in OCD (10). Dorsal frontal-striatal dysfunctions mainly concern executive processes, such as planning and conflict monitoring and emotional regulation problems in OCD. Planning strongly relies on an intact dorsal frontal-striatal circuit (premotor and dorsolateral prefrontal cortices, thalamus, and basal ganglia) and visuospatial (precuneus and parietal cortices) system. OCD patients show impaired planning performance, correlating with decreased responsiveness of the dorsal frontal-striatal circuit and enhanced recruitment of presumably compensation and stress-related brain regions, such as the anterior cingulate cortex (52). Proper functioning of the dorsal and medial prefrontal regions (e.g., the dorsal part of the anterior cingulate cortex, the medial prefrontal cortex, and the dorsolateral prefrontal cortex) is also important for the regulation of emotional responses (53,54).

OCD patients had significantly higher FA values in various white matter tracts, including the left inferior longitudinal fasciculus, bilateral superior longitudinal fasciculus, right inferior fronto-occipital fasciculus, bilateral cortico-spinal tract, corpus callosum splenium and genu, bilateral forceps major, bilateral forceps minor, left cingulum,

right uncinate fasciculus, and left cerebellar and brainstem white matter. Furthermore, symptom severity (CY-BOCS scores) correlated positively with increased FA in the left uncinate fasciculus, corticospinal tract, superior longitudinal fasciculus, forceps major, forceps minor, superior corona radiata, splenium, anterior thalamic radiation, and posterior limb of the internal capsule. These results are more extensive but broadly consistent with the findings in adult DTI studies in OCD that have reported abnormalities in the anterior limb of the internal capsule (55,56), cingulum bundle (57,58), corpus callosum (59), medial prefrontal (17,18), parietal (17,57), and occipital (57) white matter. Regarding the direction of the findings, several of the adult OCD studies reported reduced rather than increased FA in OCD compared with healthy controls (53,57,59). However, it is important to note that the adult DTI literature is characterized by small samples and varied methods. Consequently, the findings have been inconsistent and contradictory. For example, several studies also reported higher FA in adult OCD patients (18,55,56).

The finding of a positive correlation between symptom severity (CY-BOCS) and increased FA in the anterior limb of the internal capsule, the medial portion of which includes the anterior thalamic radiation carrying nerve fibers between thalamus and prefrontal cortex may be of particular theoretical and clinical relevance because it has long been hypothesized to be implicated in OCD. Adult patients with severe treatment-refractory anxiety and OCD are sometimes offered capsulotomy, an ablative surgical intervention, which employs either radiofrequency heating (thermo-capsulotomy) or gamma radiation (gamma-capsulotomy) to lesion this structure. Some patients (approximately 50%) seem to benefit from this intervention, although controlled studies have not been conducted (60). The finding of a significant FA increase in the cingulum is consistent not only with a large body of literature implicating the cingulate cortex in OCD (12) but also with the efficacy of cingulotomy for severe forms of anxiety including treatment-resistant OCD (61). The uncinate fasciculus, which connects medial temporal structures, such as the hippocampus and amygdala, with the orbitofrontal cortex is also relevant because both structures have been implicated in OCD and related emotional disorders (10).

Taken together, the implication of multiple white matter tracts in pediatric OCD is consistent not only with the traditional neurobiological model of OCD but also with recent data suggesting that brain systems, other than the hypothesized frontostriatal neural circuits, such as the parietal cortex or the limbic system, are also likely to be implicated in pediatric OCD (10,17). The findings support a developmental hypothesis of OCD that is characterized by hyperconnectivity of different brain regions. The process of brain development from childhood to adulthood is accompanied by myelination that continues into the third decade of life, particularly in the frontal lobe (62). Thus, OCD may be characterized by premature myelination. Increased FA may also reflect increased crossing fibers or less organized connectivity in participants with OCD. The specificity of these findings is unclear because many of the brain systems implicated in pediatric OCD are likely to be involved in a range of neurodevelopmental and emotional disorders. This seems logical, because many of these disorders share both genetic and environmental risk factors (63).

Limitations

The main limitation of this study is that approximately half of the sample was on medication at the time of the study, although subgroup analyses indicated that medication status did not influence the findings. We could not examine the potential impact of the various symptom dimensions of OCD because small numbers precluded meaningful examination of symptom types. It is clear, however, from a growing literature that the major symptom dimensions of the disorder are mediated by at least partially distinct neural substrates (64). Finally, the cross-sectional nature of the study does not allow firm conclusions about the causality of the reported abnormalities, whether they precede the onset of the symptoms, or whether they are a consequence of the disabling symptoms of the disorder. Longitudinal research and the study of unaffected relatives (65) may help shed some light on this question.

Conclusion

Children and adolescents with OCD display a wide range of gray matter and white matter abnormalities that are broadly consistent with those identified in the adult OCD literature but seem more extensive. Longitudinal research is necessary to determine how different developmental brain patterns are associated with the persistence of OCD, its response to treatments of various modalities, and its long-term outcome.

1. Ruscio AM, Stein DJ, Chiu WT, Kessler RC (2010): The epidemiology of obsessive-compulsive disorder in the National Comorbidity Survey Replication. *Mol Psychiatry* 15:53– 63.
2. Heyman I, Fombonne E, Simmons H, Ford T, Meltzer H, Goodman R (2001): Prevalence of obsessive-compulsive disorder in the British nationwide survey of child mental health. *Br J Psychiatry* 179:324– 329.
3. Leckman JF, Denys D, Simpson HB, Mataix-Cols D, Hollander E, Saxena S, et al. (2010): Obsessive-compulsive disorder: A review of the diagnostic criteria and possible subtypes and dimensional specifiers for DSM-V. Depression and anxiety. 27:507–527.
4. van Grootheest DS, Cath DC, Beekman AT, Boomsma DI (2005): Twin studies on obsessive-compulsive disorder: A review. *Twin Res Hum Genet* 8:450 – 458.
5. Rosario-Campos MC, Leckman JF, Mercadante MT, Shavitt RG, Prado HS, Sada P, et al. (2001): Adults with early-onset obsessive-compulsive disorder. *Am J Psychiatry* 158:1899 –1903.
6. Fontenelle LF, Mendlowicz MV, Marques C, Versiani M (2003): Early- and late-onset obsessive-compulsive disorder in adult patients: An exploratory clinical and therapeutic study. *J Psychiatr Res* 37:127– 133.
7. March JS, Franklin ME, Leonard H, Garcia A, Moore P, Freeman J, et al. (2007): Tics moderate treatment outcome with sertraline but not cognitive-behavior therapy in pediatric obsessive-compulsive disorder. *Biol Psychiatry* 61:344–347.
8. Lomax CL, Oldfield VB, Salkovskis PM (2009): Clinical and treatment comparisons between adults with early- and late-onset obsessive-compulsive disorder. *Behav Res Ther* 47:99 –104.
9. Saxena S, Rauch SL (2000): Functional neuroimaging and the neuroanatomy of obsessive-compulsive disorder. *Psychiatr Clin North Am* 23: 563–586.
10. Mataix-Cols D, van den Heuvel OA (2006): Common and distinct neural correlates of obsessive-compulsive and related disorders. *Psychiatr Clin North Am* 29:391– 410, viii.
11. Radua J, Mataix-Cols D (2009): Voxel-wise meta-analysis of grey matter changes in obsessive-compulsive disorder. *Br J Psychiatry* 195: 393– 402.
12. Radua J, van den Heuvel OA, Surguladze S, Mataix-Cols D (2010): Meta-analytical comparison of voxel-based morphometry studies in obsessive-compulsive disorder vs other anxiety disorders. *Arch Gen Psychiatry* 67:701–711.
13. Menzies L, Chamberlain SR, Laird AR, Thelen SM, Sahakian BJ, Bullmore ET (2008): Integrating evidence from neuroimaging and neu-

ropsychological studies of obsessive-compulsive disorder: The orbitofronto-striatal model revisited. *Neurosci Biobehav Rev* 32:525–549.

14. Huyser C, Veltman DJ, de Haan E, Boer F (2009): Paediatric obsessive-compulsive disorder, a neurodevelopmental disorder? Evidence from neuroimaging. *Neurosci Biobehav Rev* 33:818–830.

15. Busatto GF, Buchpiguel CA, Zamignani DR, Garrido GE, Glabus MF, Rosario-Campos MC, et al. (2001): Regional cerebral blood flow abnormalities in early-onset obsessive-compulsive disorder: An exploratory SPECT study. *J Am Acad Child Adolesc Psychiatry* 40:347–354.

16. Gilbert AR, Akkal D, Almeida JR, Mataix-Cols D, Kalas C, Devlin B, et al. (2009): Neural correlates of symptom dimensions in pediatric obsessive-compulsive disorder: A functional magnetic resonance imaging study. *J Am Acad Child Adolesc Psychiatry* 48:936–944.

17. Menzies L, Williams GB, Chamberlain SR, Ooi C, Fineberg N, Suckling J, et al. (2008): White matter abnormalities in patients with obsessive-compulsive disorder and their first-degree relatives. *Am J Psychiatry* 165:1308–1315.

18. Nakamae T, Narumoto J, Sakai Y, Nishida S, Yamada K, Nishimura T, et al. (2011): Diffusion tensor imaging and tract-based spatial statistics in obsessive-compulsive disorder. *J Psychiatr Res* 45:687–690.

19. Bora E, Harrison BJ, Fornito A, Cocchi L, Pujol J, Fontenelle LF, et al. (2010): White matter microstructure in patients with obsessive-compulsive disorder. *J Psychiatry Neurosci* 36:42–46.

20. Scahill L, Riddle MA, McSwiggin-Hardin M, Ort SI, King RA, Goodman WK, et al. (1997): Children's Yale-Brown Obsessive Compulsive Scale: reliability and validity. *J Am Acad Child Adolesc Psychiatry* 36:844–852.

21. Wechsler D (1999): *Wechsler Abbreviated Scale of Intelligence.* San Antonio, TX: The Psychological Corporation.

22. Smith SM, Jenkinson M, Woolrich MW, Beckmann CF, Behrens TE, Johansen-Berg H, et al. (2004): Advances in functional and structural MR image analysis and implementation as FSL. *Neuroimage* 23(suppl 1):S208–219.

23. Ashburner J, Friston KJ (2001): Voxel-based morphometry—The methods. *Neuroimage* 11:805–821.

24. Good CD, Johnsrude IS, Ashburner J, Henson RN, Friston KJ, Frackowiak RS (2001): A voxel-based morphometric study of ageing in 465 normal adult human brains. *Neuroimage* 14:21–36.

25. Smith SM (2002): Fast robust automated brain extraction. *Hum Brain Mapp* 17:143–155.

26. Zhang Y, Brady M, Smith S (2001): Segmentation of brain MR images through a hidden Markov random field model and the expectation-maximization algorithm. *IEEE Trans Med Imaging* 20:45–47.

27. Jenkinson M, Smith S (2001): A global optimisation method for robust affine registration of brain images. *Med Image Anal* 5:143–156.

28. Jenkinson M, Bannister P, Brady M, Smith S (2002): Improved optimization for the robust and accurate linear registration and motion correction of brain images. *Neuroimage* 17:825–841.

29. Andersson JLR, Jenkinson M, Smith S (2007): Non-linear optimisation. FMRIB technical report TR07JA1. Available at http://www.fmrib.ox.ac.uk/analysis/techrep/tr07ja1/tr07ja1.pdf.

30. Andersson J, Jenkinson, M, Smith, S (2007): Non-linear optimisation. FMRIB technical report TR07JA1 from www.fmrib.ox.ac.uk/analysis/techrep/. FMRIB, Oxford University.

31. Rueckert D, Sonoda LI, Hayes C, Hill DL, Leach MO, Hawkes DJ (1999): Nonrigid registration using free-form deformations: Application to breast MR images. *IEEE Trans Med Imaging* 18:712–721.

32. Benjamini Y, Hochberg Y (1995): Controlling the false discovery rate—A practical and powerful approach to multiple testing. *J R Statist Soc B Met* 57:289–300.

33. Patenaude B (2007): *Bayesian Statistical Models of Shape and Appearance for Subcortical Brain Segmentation* [dissertation]. Oxford: Department of Neurology, University of Oxford.

34. Cootes TF, Taylor CJ (2004): Anatomical statistical models and their role in feature extraction. *Br J Radiol* 77(spec no 2):S133–139.

35. Smith SM, Jenkinson M, Johansen-Berg H, Rueckert D, Nichols TE, Mackay CE, et al. (2006): Tract-based spatial statistics: Voxelwise analysis of multi-subject diffusion data. *Neuroimage* 31:1487–1505.

36. Smith SM, Nichols TE (2009): Threshold-free cluster enhancement: addressing problems of smoothing, threshold dependence and localisation in cluster inference. *Neuroimage* 44:83–98.

37. Rapoport JL (1990): The waking nightmare: An overview of obsessive compulsive disorder. *J Clin Psychiatry* 51(suppl):25–28.

38. Rotge JY, Langbour N, Guehl D, Bioulac B, Jaafari N, Allard M, et al. (2010): Gray matter alterations in obsessive-compulsive disorder: An anatomic likelihood estimation meta-analysis. *Neuropsychopharmacology* 35:686–691.

39. Whiteside SP, Port JD, Abramowitz JS (2004): A meta-analysis of functional neuroimaging in obsessive-compulsive disorder. *Psychiatry Res* 132:69–79.

40. Jenike MA, Breiter HC, Baer L, Kennedy DN, Savage CR, Olivares MJ, et al. (1996): Cerebral structural abnormalities in obsessive-compulsive disorder. A quantitative morphometric magnetic resonance imaging study. *Arch Gen Psychiatry* 53:625–632.

41. Singer HS, Reiss AL, Brown JE, Aylward EH, Shih B, Chee E, et al. (1993): Volumetric MRI changes in basal ganglia of children with Tourette's syndrome. *Neurology* 43:950–956.

42. Peterson B, Riddle MA, Cohen DJ, Katz LD, Smith JC, Hardin MT, et al. (1993): Reduced basal ganglia volumes in Tourette's syndrome using three-dimensional reconstruction techniques from magnetic resonance images. *Neurology* 43:941–949.

43. Rauch SL, Phillips KA, Segal E, Makris N, Shin LM, Whalen PJ, et al. (2003): A preliminary morphometric magnetic resonance imaging study of regional brain volumes in body dysmorphic disorder. *Psychiatry Res* 122:13–19.

44. Rauch SL, Savage CR, Alpert NM, Fischman AJ, Jenike MA (1997): The functional neuroanatomy of anxiety: A study of three disorders using positron emission tomography and symptom provocation. *Biol Psychiatry* 42:446–452.

45. Gilbert AR, Mataix-Cols D, Almeida JR, Lawrence N, Nutche J, Diwadkar V, et al. (2008): Brain structure and symptom dimension relationships in obsessive-compulsive disorder: A voxel-based morphometry study. *J Affect Disord* 109:117–126.

46. Alexander GE, DeLong MR, Strick PL (1986): Parallel organization of functionally segregated circuits linking basal ganglia and cortex. *Annu Rev Neurosci* 9:357–381.

47. Cummings JL (1993): Frontal-subcortical circuits and human behavior. *Arch Neurol* 50:873–880.

48. Groenewegen HJ, Uylings HB (2000): The prefrontal cortex and the integration of sensory, limbic and autonomic information. *Prog Brain Res* 126:3–28.

49. Remijnse PL, Nielen MM, van Balkom AJ, Cath DC, van Oppen P, Uylings HB, et al. (2006): Reduced orbitofrontal-striatal activity on a reversal learning task in obsessive-compulsive disorder. *Arch Gen Psychiatry* 63:1225–1236.

50. van den Heuvel OA, Veltman DJ, Groenewegen HJ, Cath DC, van Balkom AJ, van Hartskamp J, et al. (2005): Frontal-striatal dysfunction during planning in obsessive-compulsive disorder. *Arch Gen Psychiatry* 62:301–309.

51. Harrison BJ, Soriano-Mas C, Pujol J, Ortiz H, Lopez-Sola M, Hernandez-Ribas R, et al. (2009): Altered corticostriatal functional connectivity in obsessive-compulsive disorder. *Arch Gen Psychiatry* 66:1189–200.

52. van den Heuvel OA, Veltman DJ, Groenewegen HJ, Witter MP, Merkelbach J, Cath DC, et al. (2005): Disorder-specific neuroanatomical correlates of attentional bias in obsessive-compulsive disorder, panic disorder, and hypochondriasis. *Arch Gen Psychiatry* 62:922–933.

53. Bora E, Yucel M, Pantelis C (2010): Neurocognitive markers of psychosis in bipolar disorder: A meta-analytic study. *J Affective Disord* 127:1–9.

54. Ochsner KN, Gross JJ (2005): The cognitive control of emotion. *Trends Cogn Sci* 9:242–249.

55. Cannistraro PA, Makris N, Howard JD, Wedig MM, Hodge SM, Wilhelm S, et al. (2007): A diffusion tensor imaging study of white matter in obsessive-compulsive disorder. *Depress Anxiety* 24:440–446.

56. Yoo SY, Jang JH, Shin YW, Kim DJ, Park HJ, Moon WJ, et al. (2007): White matter abnormalities in drug-naive patients with obsessive-compulsive disorder: A diffusion tensor study before and after citalopram treatment. *Acta Psychiatr Scand* 116:211–219.

57. Szeszko PR, Ardekani BA, Ashtari M, Malhotra AK, Robinson DG, Bilder RM, et al. (2005): White matter abnormalities in obsessive-compulsive disorder: A diffusion tensor imaging study. *Arch Gen Psychiatry* 62:782–790.

58. Ha TH, Kang DH, Park JS, Jang JH, Jung WH, Choi JS, et al. (2009): White matter alterations in male patients with obsessive-compulsive disorder. *Neuroreport* 20:735–739.

59. Garibotto V, Scifo P, Gorini A, Alonso CR, Brambati S, Bellodi L, et al. (2010): Disorganization of anatomical connectivity in obsessive compulsive disorder: A multi-parameter diffusion tensor imaging study in a subpopulation of patients. *Neurobiol Dis* 37:468–476.

60. Ruck C, Karlsson A, Steele JD, Edman G, Meyerson BA, Ericson K, *et al.* (2008): Capsulotomy for obsessive-compulsive disorder: Long-term follow-up of 25 patients. *Arch Gen Psychiatry* 65:914–921.

61. Baer L, Rauch SL, Ballantine HT, Jr., Martuza R, Cosgrove R, Cassem E, *et al.* (1995): Cingulotomy for intractable obsessive-compulsive disorder. Prospective long-term follow-up of 18 patients. *Arch Gen Psychiatry* 52:384–392.

62. Giorgio A, Watkins KE, Chadwick M, James S, Winmill L, Douaud G, *et al.* (2010): Longitudinal changes in grey and white matter during adolescence. *Neuroimage* 49:94–103.

63. Lichtenstein P, Carlstrom E, Rastam M, Gillberg C, Anckarsater H (2010): The genetics of autism spectrum disorders and related neuropsychiatric disorders in childhood. *Am J Psychiatry* 167:1357–1363.

64. van den Heuvel OA, Remijnse PL, Mataix-Cols D, Vrenken H, Groenewegen HJ, Uylings HB, *et al.* (2009): The major symptom dimensions of obsessive-compulsive disorder are mediated by partially distinct neural systems. *Brain* 132:853–868.

65. Chamberlain SR, Menzies L (2009): Endophenotypes of obsessive-compulsive disorder: Rationale, evidence and future potential. *Expert Rev Neurother* 9:1133–1146.